

Micro-Cogeneration with a Fresnel Solar Concentrator

Marco Bortolini¹, Mauro Gamberi², Alessandro Graziani^{1,2}

¹Department of Industrial Engineering, University of Bologna, Viale del Risorgimento 2, 40136, Bologna - Italy

²Department of Management and Engineering, University of Padova, Stradella San Nicola 3, 36100, Vicenza - Italy

Abstract:- The technical and economic sustainability of photovoltaic (PV) systems is heavily affected by the cost and performances of the adopted PV cells. Solar concentrators represent an effective alternative to reduce the solar cell surface and, at the same time, to increase the global conversion efficiency. Such systems include optic elements to concentrate the solar radiation to a small area where high-efficiency PV cells are located. Particularly, the adoption of multi-junction cells, e.g. Triple-Junction Photovoltaic (TJPV) cells, is encouraged to increase the power conversion performance. This paper presents full details about the design and operating features of a Fresnel lens solar concentrator for the micro-cogeneration of electrical power and thermal energy. The two axis controlled prototype integrates five different functional modules to guarantee the required features. Basically, the TJPV cells allow power production, while eight Water Heat Exchangers (WHEs) are installed for both the cell cooling and the recovery of thermal energy. The operative concentration factor is up to 800x through eight non-imaging Fresnel lenses integrated to the solar collector. Furthermore, a two axes solar tracker assures sun collimation during day-time. The prototype control, together with the monitoring of the environmental conditions and the energy conversion performances, is provided thanks to a semi-automatic real-time interface developed adopting LabView© Integrated Development Environment (IDE). A set of preliminary field-tests is assessed to study both the solar collimation accuracy and the prototype overall energy performances. The obtained evidences are presented and fully discussed in this paper.

Keywords:- concentrator system, distributed micro-cogeneration, Fresnel lens, solar energy, solar tracking.

I. INTRODUCTION

Photovoltaic (PV) silicon solar cells generally produce electricity with a conversion efficiency lower than 26% [1], while multi-junction solar cells, III-V components based, reach values close to 42% [2][3] and represent, nowadays, a performing solution to convert the sun rays to power energy. Unfortunately, due to their high cost, these cells are not convenient for standard flat-plane modules. Crystalline silicon represents, actually, the most adopted material to produce PV modules. The concentrating solar technology allows to reduce the receiver surface due to the concentration of the sun rays to a small area, i.e. focus point. Consequently, in such energy plants, the adoption of multi-junction solar cells becomes feasible and potentially profitable [4]. Zubi et al. [5] present the state of the art of high concentration photovoltaics. These energy conversion systems adopt parabolic mirrors or lenses to convey the sun rays to the solar receiver. El Gharbi et al. [6] analyze and compare such optic technologies, while Xie et al. [7] and Chemisana et al. [8] focus and review the applications integrating Fresnel lenses. Sonneveld et. al [9] and Chemisana [10] review and describe building integrated concentrating PV systems highlighting the current state of the art and the possible future scenarios.

Solar concentration systems generally require a cooling circuit to control the receiver temperature preventing damages to the cells and the decrease of their conversion efficiency level. Chemisana et al. [11] estimate an average decrease of the cell electrical performances equal to 0.14% per Celsius degree. Even if a cooling hydraulic circuit is often necessary, nowadays, few applications integrate a thermal recovery unit to solar concentrators. Combined heat and power (CHP) systems are not often developed, especially for small size solar energy systems, i.e. micro-cogeneration, while a large number of contributions consider CHP plants integrated to plane modules. Immovilli et al. [12] focus this aspect in deep. Finally, solar concentrators are able to capture only the beam fraction of the solar radiation. A sun tracking system represents a crucial device to increase the solar conversion efficiency. Aim of this device is to guarantee the best collimation between the solar collector and the sun, from sunrise to sunset, so that the former is always orthogonal to the direction of the sun rays [13]. Bortolini et al. describe the design and test of a sun tracking system based on a feedback control algorithm applied to a Fresnel lens small scale module [14][15].

Aim of this paper is to present the design, development and field-test of a solar concentrating prototype for the distributed micro-cogeneration of heat and power. The system integrates a solar collector, to concentrate the solar radiation, a set of eight receivers, including high efficiency triple junction photovoltaic (TJPV) cells, for power generation, and a same number of water heat exchangers (WHEs) for the cell cooling and the thermal recovery. To increase the global conversion efficiency, a biaxial solar tracker is installed and properly controlled.

The developed energy system allows to study the electric and thermal conversion efficiencies together with an assessment of the solar collimation accuracy. Furthermore, an analysis of the expected manufacturing costs highlights the crucial drivers affecting an investment in such solar energy plants.

The reminder of this paper is organized as follows: the next Section 2 describes the developed prototype, giving full details about its functional modules. Section 3 introduces the aforementioned economic analysis of the system manufacturing costs, while, in Section 4, the outcomes of a set of field-tests are discussed highlighting the perspectives for such an energy system. Conclusions are drawn in Section 5 together with suggestions for further research and the prototype improvement.

II. SOLAR CONCENTRATOR PROTOTYPE DESCRIPTION

The following Figure 1 shows a picture of the developed prototype.

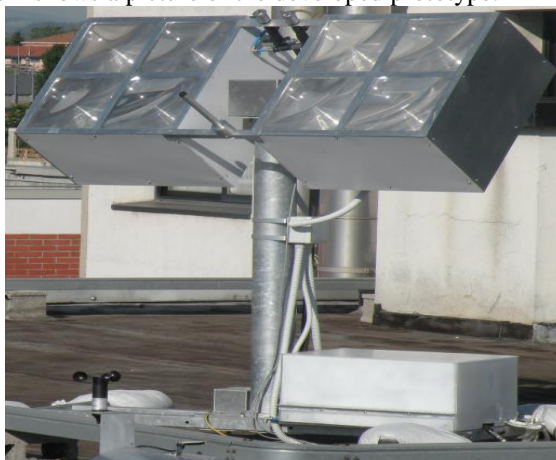


Fig. 1: Developed Fresnel solar prototype

The overall dimensions are, approximately, of 1.6x1.7x2m height and the weight is of 120kg. The solar conversion system allows the CHP production due to the refraction of solar radiation. A set of eight squared 330x330mm Fresnel lenses, fixed on a reticular frame, made of several welded aluminum squared profiles, i.e. the solar collector, concentrates the incident radiation on an equivalent number of solar receivers located in correspondence of the lens foci. Each of them includes a high efficiency TJPV solar cell installed on a WHE with the purpose of both cell cooling and thermal recovery. Furthermore, the biaxial solar tracker guarantees the highest captation of solar radiation during the day by aligning the system position to the direction of the incident sun rays. The solar tracker consists of two mechanical actuators able to rotate both the collector and the receiver along two solar coordinates, i.e. the azimuthal and zenithal axes of motion, so that the surface of the Fresnel lenses, i.e. the solar collector, is always orthogonal to the direction of the incident radiation. An electronic remote controller implements a closed loop algorithm for solar tracking. At last, the hydraulic circuit integrated to the prototype allows the cooling of the cells and the heat recovery supplying the cooling fluid, i.e. purified water, to the WHEs.

The following five functional modules are integrated to the prototype:

- support steel structure;
- solar collector and receivers;
- solar tracking system;
- real-time motion control and monitoring system;
- hydraulic circuit for cell cooling and thermal recovery.

Further details about each of them are provided in the next paragraphs of this Section together with a quantitative description of the design choices.

2.1 Support steel structure

The support structure of the developed prototype is made of two elements, both realized with galvanized steel, i.e. the support base and the vertical pillar (see Figure 1). The former, whose dimensions are 1.6x1.0m, prevents the tip over of the whole plant and it is made of four squared 50x50mm welded tubular profiles. A 320x320mm galvanized steel plate is screwed in the centre of the base and supports the latter

structural element, i.e. the vertical pillar. Its height is of 1.4m and the diameter of 140mm. On top of the pillar it is located a 1.6m horizontal shaft supporting the reticular solar collector, integrating the Fresnel lenses and the receivers.

2.2 Solar collector and receivers

The designed solar collector detects the incident radiation on a wide surface and concentrates it to a smaller area, i.e. the focus point, where the receivers, including the TJPV solar cells, are located. The ratio between the collector and the receiver areas is known as the geometric concentration factor. The developed prototype includes eight different collector + receiver modules. Each of them integrates a commercial 330×330mm PMMA Fresnel lens and an aluminium WHE with up to four 10×10mm InGa/GaAs/Ge TJPV cell ($\eta_{nom} = 35\%$ measured in standard temperature and irradiation conditions). Figure 2 shows a picture and a 3D render of the described receiver. The electric and hydraulic connections of both the cells and the WHEs are in series, while the maximum lens concentration factor is of 800x.

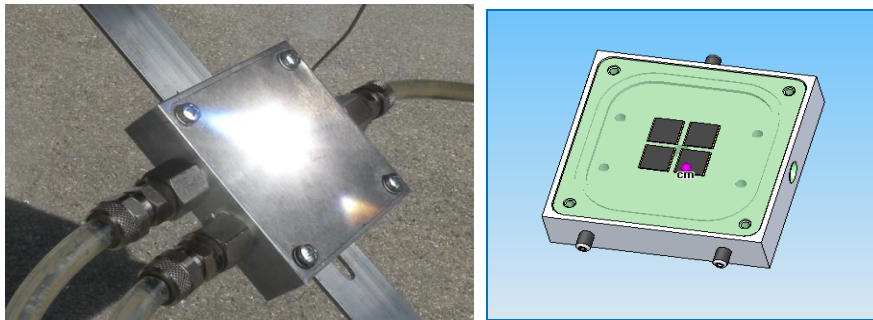


Fig. 2: Solar receiver integrating the TJPV solar cells

Each WHE presents one entry and two exits holes and its design increases the heat exchange between the cooling fluid and the aluminium plate where the cell is fixed. The inlet flow hits perpendicularly the portion of the WHE surface where the TJPV cell is located, while the exit holes are laterally located. The overall heat exchange surface is, approximately, of 64cm².

To correctly support both the lenses and the receivers a metallic reticular structure is designed. Two frames are realized. Each of them integrates four modules and its dimensions are of 666×666×400mm, accordingly to the Fresnel lens size and their focal distance, equal to 350mm. Finally, a set of metal panels, located on bottom and lateral surfaces of each frame, protects the receivers preventing damages.

2.3 Solar tracking system

To maximize the captation of the solar radiation, the solar tracking system guarantees an accurate collimation between the prototype and the sun during the whole day. Two distinct cinematic mechanisms assure the biaxial motion of the prototype. Both mechanisms adopt a stepper motor as the actuator. Its holding torque is of 3Nm, the phase current of 4.2A DC and the angular step resolution is of 1.8 degrees. Each actuator is coupled to a gear reducer (gear ratio equal to 100) and to a further chain drive motion transmission system (gear ratio equal to 4) as in Figure 3. Globally, the angular resolution is close to 10⁻³ degrees per step. The tracking mechanisms are installed in two different positions: for the zenithal axis of motion the tracker is located on a plate on top of the pillar and it is directly coupled to the shaft that supports the reticular frames containing the lenses and the receivers. On the contrary, the azimuthal tracker is close to the bottom of the vertical pillar and the transmission of motion is made thanks to a vertical shaft coaxial to the pillar and placed inside it. Finally, a real time remote controller, implementing the closed loop algorithm described in the following, manages the motion control. Two metal capsules are used to protect each tracking mechanism from the rain and other atmospheric agents.

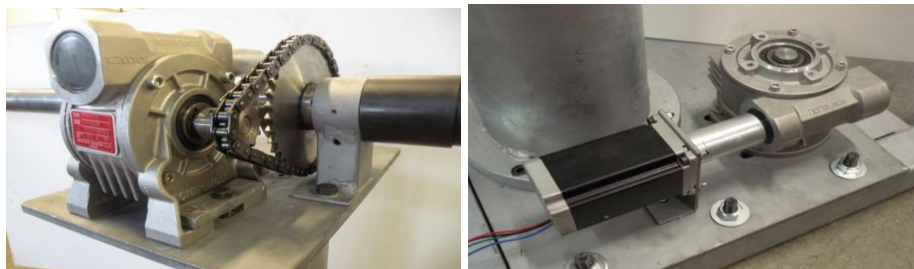


Fig. 3: Zenithal and azimuthal tracking mechanisms

2.4 Real-time motion control and monitoring system

The developed prototype integrates a real-time remote control platform for the biaxial regulation and the cyclic measure of both the environmental conditions and the energy conversion parameters. Such a platform is developed with LabView© Integrated Development Environment (IDE) and it runs on a NI C-RIO real-time auxiliary industrial module. The next Figure 4 proposes the key concept of the feedback loop to control the zenithal and azimuthal motion axes.

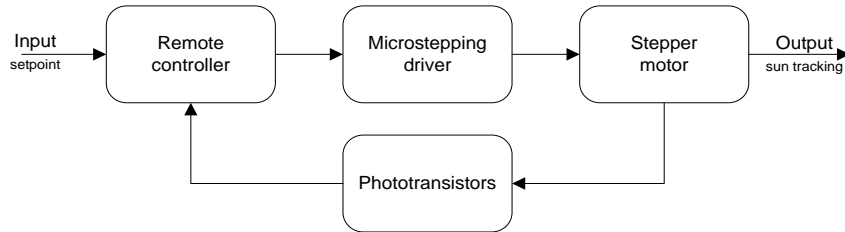


Fig. 4: Feedback control loop adopting phototransistors

The remote controller implements an iterative algorithm based on the difference between the transduced current signals, measured by a set of four phototransistors used as solar irradiance sensors, and properly integrated to the solar collimator represented in the next Figure 5. For each motion axis, the difference between the transduced signals is correlated to the misalignment between the sun rays and the current system position. As a consequence, if the alignment gap is out of a given tolerance the system needs to be realigned. The microstepping driver modulates the power signal of a 24 V DC generator and it supplies the stepper motors rotating the solar collector until the alignment gap is back to the defined tolerance range. The angular resolution of about 10^{-3} degrees per step assures high accuracy in daily sun collimation. Further details about the real-time control strategy are in Bortolini et al. [14][15].

The remote controller further monitors the most relevant environmental and energetic parameters to evaluate the plant performances and to calculate the aggregate power and thermal conversion efficiencies. The profiles of the global and beam radiation, the air temperature, the wind speed and direction are traced together with the produced electrical power and the recovered thermal energy.



Fig. 5: Solar collimator for biaxial tracking

Figure 6 shows the auxiliary weather station adopted to monitor the major weather parameters and the pyr heliometer for the beam radiation measure. Details about the adopted sensors are in Table I.



Fig. 6: Weather station and the pyr heliometer

Table I: Features of the adopted environmental sensors

Sensor	Details	Adopted operative range	Output signal range
--------	---------	-------------------------	---------------------

Pyranometer	Delta Ohm - LP Pyra 03AC Sensitivity: 17.09mV/(kW/m ²) Impedance: 37.6Ω	0..2000W/m ²	4..20mA
Pyrheliometer	Kipp & Zonen - CHP1, AMPBOX Sensitivity: 8.03μV/(kW/m ²) Impedance: 30.3Ω	0..1600W/m ²	4..20mA
Air thermometer	Italcoppie Pt-100, Transmitter Accuracy: ±0.12Ω at 0°C	-12..47°C	4..20mA
Anemometer	BitLine - Anemometer, Transmitter Speed sensitivity: 1km/h Direction sensitivity: 10 degrees	Speed: 0..150km/h Direction: 0..360degrees	Speed: 4.20mA Direction: 4..20mA

2.5 Hydraulic circuit and thermal recovery unit

The hydraulic circuit, represented in the next Figure 7, both cools the TJPV cells and recover thermal energy. It mainly deals of two closed loops integrating four WHEs each. The cold fluid flows through the WHEs thanks to a magnetic driver gear pump. The flow rate is remotely controlled in the range 500÷5000rpm. At the end of the loop, the hot fluid reaches a brazed 14 plates heat exchanger (plate surface area of 0.03m²) for the heat recover. The water flowing in the second cooling loop and directly feeding the users is heated and it flows thanks to a further circulation gear pump. In Figure 7, for the sake of simplicity, the users are exemplified by a tank. Inlet and outlet temperatures in several stages of the circuit are measured through a set of PT100 temperature sensors, while a low volume rotating vane flow meter measures the flow rate. The acquired signals are processed by the real time remote control system described in previous Paragraph 2.4. Finally, the hydraulic circuit integrates a two litres expansion vessel, two dearators and a safety valve calibrated to prevent the pressure to become higher than 0.15MPa.

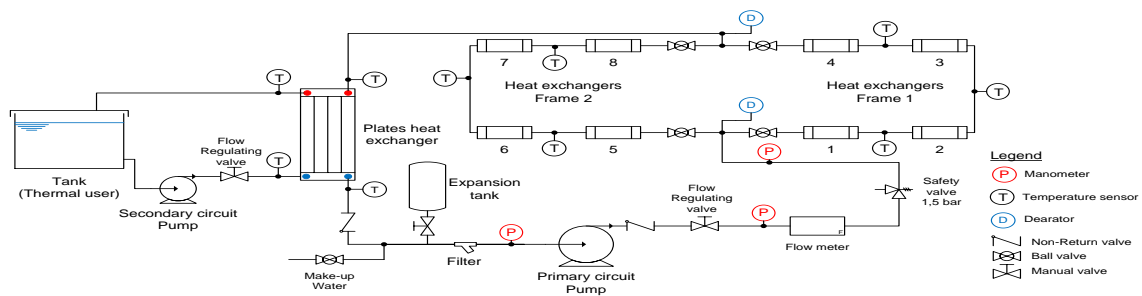


Fig. 7: Hydraulic circuit for cell cooling and thermal recovery

III. MANUFACTURING COST ANALYSIS

Despite the proposed prototype is at a research stage of its life cycle and, consequently, it is far from an optimized large scale production, a realistic analysis of the rising manufacturing costs is, already, feasible. Such costs represent the initial investment in a solar energy system like the described prototype. A functional perspective drives the analysis of the rising costs. Direct materials and labour costs are computed separately. Table II and Figure 8 summarize the key data.

Table II: Prototype manufacturing costs

Description	# units/kg	Total cost [€]
TJ-PV cells	8 units	36.00
Fresnel lenses	8 units	96.00
Sun tracking system		469.00
<i>Gear reducer</i>	2 units	
<i>Chain drive system</i>	2 units	
<i>Stepper motor</i>	2 units	
<i>Microstepping driver</i>	2 units	
Support structure		92.00
<i>Galvanized steel structure (base, pillar and shaft)</i>	40kg	

Micro-Cogeneration with a Fresnel Solar Concentrator

<i>Aluminum frames (collector)</i>	<i>8kg</i>	
Hydraulic circuit		293.20
<i>Circulation pump</i>	<i>1 unit</i>	
<i>Heat exchangers</i>	<i>8 units</i>	
<i>Plate heat exchanger</i>	<i>1 unit</i>	
<i>Deareator</i>	<i>1 unit</i>	
<i>Expansion vassel</i>	<i>1 unit</i>	
<i>Filter</i>	<i>1 unit</i>	
<i>Piping</i>	<i>1 unit</i>	
Direct labor cost		200.00
Full production cost		1186.20

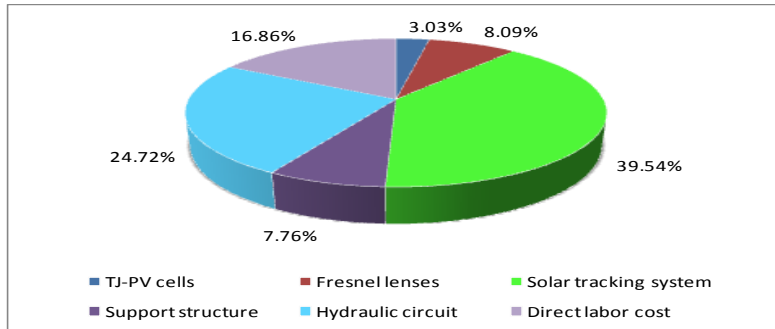


Fig. 8: Functional cost analysis, percentages refer to the full manufacturing cost

The solar tracking system and the hydraulic circuit are the two functional modules with the highest impact on the system global cost. However, such modules allow to track the sun and to recover thermal energy significantly increasing the power and thermal conversion efficiencies. A trade-off analysis between the performances of flat plane PV systems and CHP concentrators is necessary to study if the increase of the conversion efficiency and energy production justify the CHP plant higher cost. Such an analysis represents a possible future development of the present paper.

IV. FIELD-TESTS AND EXPERIMENTAL CAMPAIGN

An experimental campaign to field-study the proposed prototype is assessed during the 2012 summer months in Bologna, Italy (latitude 44.51° North, longitude 11.32° East). Three different tests are developed. At first, the accuracy in sun collimation is analysed as a key condition not to decrease the amount of the collected solar radiation. The second test focuses on the analysis of a single TJPV cell studying its electric features and curves when integrated to the proposed prototype. Finally the system global conversion efficiency is investigated. The key outcomes for each experimental campaign are discussed in the next paragraphs.

4.1 Accuracy in solar tracking

The accuracy of the adopted solar tracking system heavily affects the energy conversion efficiency. In particular, the electric performance of the TJPV cells strongly depends on the uniformity of the concentrated radiation on the cell surface and a significant performance decrease happens in case of a non-homogenous distribution of the solar irradiance flux. Therefore, the feedback loop tracking strategy proposed in the previous Paragraph 2.4 is field-tested to experimentally investigate its performances in solar collimation. The measure of the shadow length generated by the collimator stem allows to calculate the angular alignment gap between the sun and the prototype. Figure 9 clarifies such a concept.

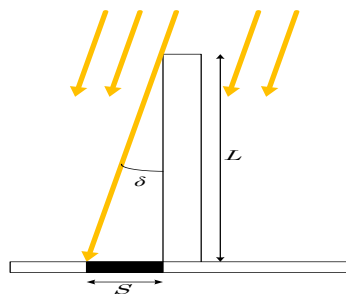


Fig. 9: Accuracy in solar collimation, shadow related to the angular misalignment

Eq. 1 correlates the angular misalignment between the sun rays and the solar collector, δ , to the shadow and the stem length.

$$\delta = \tan^{-1}\left(\frac{S}{L}\right) \quad (1)$$

Furthermore, Figure 10 shows two pictures of the solar collimator taken immediately before and after the actuator switch on, i.e. when the gap is maximum and minimum.

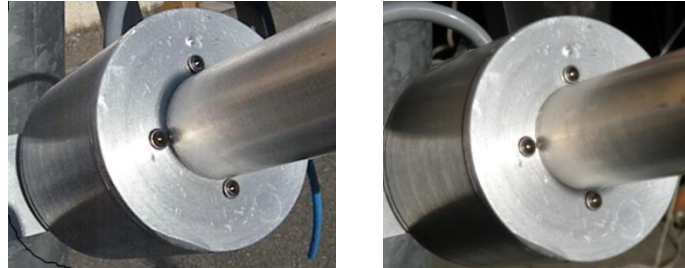


Fig. 10: Shadow before and after the system realignment

The average experimental alignment gap is lower than 0.8° representing an acceptable value according to the optical properties of the adopted Fresnel lenses.

4.2 TJPV cell electric features

The present second field-test focuses on the analysis of the energy conversion performances of a single TJPV cell when integrated to the proposed prototype. A set of runs to calculate the experimental I-V, i.e. current-voltage, and P-V, i.e. power-voltage, curves are assessed under the environmental irradiance conditions represented in the graph of Figure 11. Particularly, the red curve refers to the global radiation on the horizontal plane, while the blue one shows the beam fraction on an optimally oriented surface. The monitored parameters also include the air temperature and the wind speed and direction. During the test, 31.5°C and light wind are measured.

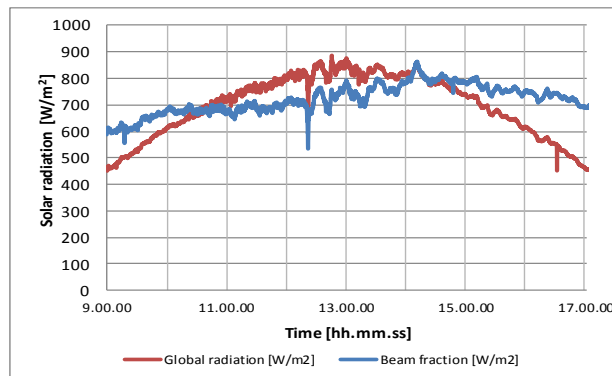


Fig. 11: Daily global and beam irradiance measured during TJPV cell analysis

The graph in Figure 12 shows a significant example of the experimental I-V and P-V curves for a single TJ-PV solar cell integrated to the Fresnel lens prototype. Particularly, the adopted cell extracts a maximum power of 8.7W when irradiated with a 800x concentrated solar radiation, while the cell conversion efficiency is equal to 15.8%.

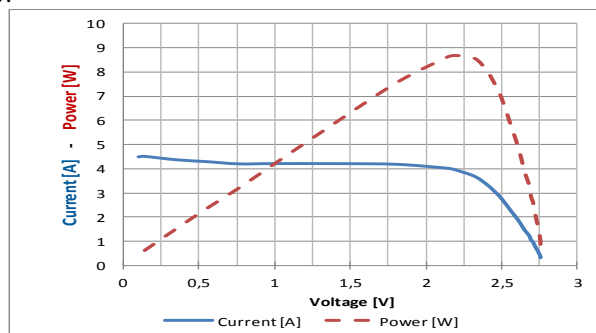


Fig. 12: Experimental I-V and P-V curves for a single TJPV cell integrated to the prototype

4.3 Global conversion efficiency analysis

During the third field-test the study of both the prototype power and thermal recovery performances is assessed. In such test, for the sake of simplicity, only one of the two frames used as solar collectors, is considered. Consequently, a series of four TJ-PV cells, fixed on a same number of heat exchangers, is adopted. The following Table III summarizes the key results of two of the most relevant runs.

The experienced electrical conversion efficiency is of about 13%, while the thermal conversion efficiency is higher than 70% and it increases to 88.65% if the flow rate is higher even if the outlet fluid temperature is lower.

The low value for the power efficiency is due to several causes. Among them the most relevant is the high dispersion of the concentrated radiation around the focus points. Therefore, the adoption of a single concentration optics, i.e. the aforementioned Fresnel lenses, is not adequate, by itself, to reduce the width of the concentrated light spot that, generally, is higher than the cell surface. Consequently, a fraction of the concentrated solar radiation does not hit the cell surface, reducing the electrical conversion efficiency and increasing the thermal energy collected by the receivers. To overcome such a weakness a secondary optics could be of help to increase the concentrated radiation acceptance angle with a foreseeable raise of the light flux hitting the cell and to increase, at the same time, the light flux distribution on the cell area. Such an improvement represents a further development for the proposed prototype.

Table III: Prototype power and thermal performances

<i>Test #1</i>					
Power generation			Thermal recovery		
Direct radiation	779	W/m ²	Flow rate	0.252	l/min
Collector area	0.3249	m ²	Inlet temperature	28.2	°C
Incident direct radiation	253.10	W	Outlet temperature	38.3	°C
Produced electrical power	30.70	W	Recovered thermal power	177.57	W
<i>Power conversion efficiency</i>	<i>12.13%</i>		<i>Thermal conversion efficiency</i>	<i>70.16%</i>	
<i>Test #2</i>					
Power generation			Thermal recovery		
Direct radiation	740	W/m ²	Flow rate	0.47	l/min
Collector area	0.3249	m ²	Inlet temperature	26.0	°C
Incident direct radiation	240.43	W	Outlet temperature	32.5	°C
Produced electrical power	31.00	W	Recovered thermal power	213.14	W
<i>Power conversion efficiency</i>	<i>12.89%</i>		<i>Thermal conversion efficiency</i>	<i>88.65%</i>	

Considering the thermal recovery performances, the field-tests highlight acceptable values for such a parameter. From a realistic point of view, such performances are affected by two major phenomena. The former is the high air temperature experienced during the tests, preventing the cooling fluid heat dispersion through the pipelines. The latter is related to the aforementioned distribution of the concentrated radiation around the focus point and, particularly, to the rays falling out of the cell surface. Such a fraction of the concentrated radiation is totally available for heat recovery because it directly hits the heat exchanger surface without the cell intermediate surface. The introduction of the secondary optics and other devices/strategies to increase the power conversion efficiency, probably, generates a parallel decrease of the thermal performances. However, the global conversion efficiency trend, i.e. electrical + thermal, should increase.

V. CONCLUSIONS AND FURTHER RESEARCH

A biaxial Fresnel solar prototype for the distributed micro-cogeneration of heat and power is designed, developed and preliminary field-tested. The system allows the production of electrical and thermal energy from the renewable solar source through the innovative concentrating technology. Details about the design choices of the five functional modules composing to the prototype are provided to study their technical features and their economic impact on the total manufacturing cost. Furthermore, a preliminary set of field-tests is conducted during the 2012 summer months in Bologna, Italy. The main purposes of such an experimental campaign are to verify the accuracy in sun collimation and to evaluate the electrical and thermal conversion efficiency of both a single InGa/GaAs/Ge multi-junction solar cell and of the whole prototype.

Experimental outcomes highlight an average alignment gap between the sun and the prototype solar collector lower than 0.8°, representing an acceptable value according to the optical properties of the adopted Fresnel lenses. Focusing on the conversion performances, both the electric efficiency of a single solar cell and of

a series of four cells, connected in series, are investigated. In the former test, developed to characterize a single TJPV cell, the produced power is of 8.7W, while the electrical conversion efficiency is equal to 15.8%. In the latter test, results highlight an electrical conversion efficiency of about 13%, while the thermal conversion efficiency depends on the cooling fluid flow rate and outlet fluid temperature. The thermal conversion performance ranges between 70% and 89%.

Further prototype developments mainly deal with the increase of the prototype electric efficiency. A secondary optics is certainly of help to increase the concentrated radiation acceptance angle raising the light flux hitting the cell and the improving its distribution on the cell surface. Finally, the obtained experimental results and performances can be related to the manufacturing and operative costs to conclude about the technical and economic profitability of the concentrating technology when integrated to concentrated systems oriented to the distributed micro-cogeneration from the solar energy source.

ACKNOWLEDGMENT

The authors would like to thank the *Fondazione Cassa di Risparmio di Trento e Rovereto* for its significant support to the project.

REFERENCES

- [1]. M.A. Green, K. Emery, Y. Hishikawa, W. Warta, "Solar cell efficiency tables (version 36)", *Progress in photovoltaics: research and applications*, 18, 346-352, 2010.
- [2]. W. Guter, J. Schone, S.P. Philipps, M. Steiner, G. Siefer, A. Wekkeli, E. Welser, E. Oliva, A.W. Bett, F. Dimroth, "Current-matched triple-junction solar cell reaching 41.1% conversion efficiency under concentrated sunlight", *Applied Physics Letters*, 94(22), 1-3.
- [3]. J.W. Pan, J.Y. Huang, C.M. Wang, H.F. Houg, Y.P. Liang, "High concentration and homogenized Fresnel lens without secondary optics element", *Optics communications*, 284, 4283-4288, 2011.
- [4]. S.R. Wenham, M.A. Green, M.E. Watt, R. Corkish, "Applied photovoltaics", *Earthscan*, London, 2007.
- [5]. G. Zubi, J. Bernal-Agustín, G.V. Fracastoro, "High concentration photovoltaic systems applying III-V cells", *Renewable and Sustainable Energy Reviews*, 13, 2645-2652, 2009.
- [6]. N. El Gharbi, H. Derbal, S. Bouaichaoui, N. Said, "A comparative study between parabolic trough collector and linear Fresnel reflector technologies", *Energy procedia*, 6, 565-572, 2011.
- [7]. W.T. Xie, Y.J. Dai, R.Z. Wang, K. Sumathy, "Concentrated solar energy applications using Fresnel lenses: A review", *Renewable and Sustainable Energy Reviews*, 15, 2588-2606, 2011.
- [8]. D. Chemisana, M. Ibáñez, J. Barrau, "Comparison of Fresnel concentrators for building integrated photovoltaics", *Energy conversion and management*, 50, 1079-1084, 2009.
- [9]. P.J. Sonneveld, G.L.A.M. Swinkels, B.A.J. Van Tuijl, H.J.J. Janssen, J. Campen, G.P.A. Bot, G.P.A., "Performance of a concentrated photovoltaic energy system with static linear Fresnel lenses" *Solar energy*, 85, 432-442., 2011.
- [10]. D. Chemisana, "Building Integrated Concentrating Photovoltaics: A review", *Renewable and Sustainable Energy Reviews*, 15, 603-611, 2011.
- [11]. D. Chemisana, M. Ibáñez, J.I. Rosell, "Characterization of a photovoltaic-thermal module for Fresnel linear concentrator", *Energy conversion and management*, 52, 3234-3240, 2011.
- [12]. F. Immovilli, A. Bellini, C. Bianchini, G. Franceschini, "Solar trigeneration for residential applications, a feasible alternative to traditional microcogeneration and trigeneration plants", *IEEE Industry Applications Society Annual Meeting*, 1-8, 2008.
- [13]. V.D. Rumyantsev, V.P. Khvostikov, O.A. Khvostikova, P.Y. Gazaryan, N.A. Sadchikov, A.S. Vlasov, E.A. Ionova, V.M. Andreev", "Structural features of a solar TPV systems", *6th conference on thermophotovoltaic generation of electricity*, Friburg, 2004.
- [14]. M. Bortolini, M. Gamberi, R. Accorsi, R. Manzini, C. Mora, A. Regattieri, "Sun tracking system design and testing for solar energy conversion systems", *Proceedings of XV Summer School Francesco Turco, Impianti Industriali Meccanici, Monopoli Bari*, 257-262, 2010.
- [15]. M. Bortolini, M. Gamberi, A. Graziani, M. Manfroni, "An Hybrid Strategy for the Bi-Axial Sun Tracking of Solar Energy Conversion Systems", *Journal of Control Engineering and Technology*, Vol.2 Issue 4, 130-142, 2012.